Journal of Magnetism and Magnetic Materials 380 (2015) 246–250

Contents lists available at ScienceDirect

Journal of Magnetism and Magnetic Materials

journal homepage: www.elsevier.com/locate/jmmm

Depth limitations for *in vivo* magnetic nanoparticle detection with a compact handheld device

Martijn Visscher, Sebastiaan Waanders, Joost Pouw, Bennie ten Haken *

MIRA Institute for Biomedical Technology and Technical Medicine, University of Twente, Drienerlolaan 5, 7522 NB Enschede, The Netherlands

ARTICLE INFO

Article history:
Received 28 June 2014
Received in revised form
12 September 2014
Accepted 29 September 2014
Available online 11 October 2014

Keywords:
Nonlinear susceptibility
Magnetic nanoparticle
Biomedical sensing
Diamagnetism of tissue
In vivo detection
Intraoperative sentinel lymph node detection

ABSTRACT

The increasing interest for local detection of magnetic nanoparticles (MNPs) during clinical interventions requires the development of suitable probes that unambiguously detect the MNPs at a depth of several centimeters in the body. The present study quantitatively evaluates the limitations of a conventional magnetometry method using a sinusoidal alternating field. This method is limited by the variability of the magnetic susceptibility of the surrounding diamagnetic tissue. Two different sensors are evaluated in a theoretical model of MNP detection in a tissue volume. For a coil that completely encloses the sample volume, the MNPs can be detected if the total mass contributing to the signal is larger than 4.1×10^{-7} times the tissue mass. For a handheld surface coil, intended to search for the MNPs in a larger tissue volume, an amount of 1 μg of iron oxide cannot be detected by sensors with a diameter larger than 15 mm. To detect a spot with MNPs at 5 cm depth in tissue, it should contain at least 325 μg iron oxide. Therefore, for high-sensitive clinical MNP detection in surgical interventions, techniques with increased specificity for the nonlinear magnetic properties of MNPs are indispensable.

1. Introduction

Alternating field magnetometry has been widely applied for magnetic analysis and measurements of MNPs. Compared to MRI and magnetic particle imaging, which require high fields and large systems, the principle of alternating field magnetometry is very suitable for clinical interventions, since it can operate at relatively low field amplitudes using simple technology. A few clinical applications for MNP detection, like sentinel lymph node detection, are based on the use of a detection coil and a single, sinusoidal excitation field [1,2].

In the last decade, several studies have been published about the application of magnetic nanoparticles (MNPs) for sentinel lymph node biopsy (SLNB) [3–8,1,2]. Especially the disadvantages accompanying the usually applied radionuclides in SLNB, concerning radiation exposure, complicated logistics and legislation, have stimulated the search for other tracers and detection methods, leading to the introduction of MNPs in SLNB. Adequate depth sensitivity of an MNP probe is crucial in this case, because axillary sentinel lymph nodes can be found to be 1.5–8 cm deep in the body [9]. A simple, unambiguous method of magnetic detection is regarded to be essential for clinical users to assist with real time information during SLN localization and resection. To realize this, the availability of sensitive handheld probes with a high MNP specificity is required.

With methods based on sinusoidal alternating field excitation (further in this paper mentioned as conventional alternating field magnetometry), the magnetic susceptibilities of the sample materials are the basis of contrast. Detection of MNPs with a large susceptibility is successful when its signal provides a good contrast with the surrounding medium with a low magnetic susceptibility, *i.e.* the tissue. However, the weight of contributions of materials with different (dimensionless) susceptibilities is based on the volume or the mass ratio. In other words, for a certain mass of MNPs, the measured signal equals the signal contribution of the tissue or the medium mass. This ratio determines the detectability of MNPs in a typical application. Therefore, for high-sensitive, clinical MNP detection, the intrinsic linear magnetic properties of the body have to be taken into account.

Conventional alternating field magnetometry also detects the linear magnetic tissue. Especially for applications with a relatively large contribution from tissue volumes and very low amounts of MNPs or MNPs at distant locations, the detection limits for MNPs are crucial. For a very low response from deeply located MNPs or a small amount of MNPs, the tissue response can dominate over the particle response. Simply increasing the excitation field strength, to increase the depth sensitivity of the sensor, will not solve the problem, since the signal-to-noise-ratio will decrease by an increased contribution of a larger tissue area. Furthermore, safety

* Corresponding author at: P.O. Box 217, 7500 AE, Enschede, The Netherlands.
E-mail address: b.tenhaken@utwente.nl (B. ten Haken).

http://dx.doi.org/10.1016/j.jmmm.2014.09.076
0304-8853/

limits on the field amplitude, heat dissipation and sensor stability may affect the clinical usability of the probe.

In this study, the intrinsic limitations of conventional alternating field magnetometry are quantitatively demonstrated for clinical MNP detection. To achieve a result that can be compared in fairness with other optimized magnetic detection techniques, the analysis is based on general and the most optimistic assumptions. The evaluation is based on two different sensor types. In model A, the MNP detection limit is calculated for a sample enclosing detection coil. Model B evaluates MNP detection in a large tissue volume with a surface coil.

2. Methods

The sensors in models A and B, both consisting of an excitation coil and a single detection coil, are quantitatively evaluated in a theoretical model. The evaluation is based on some general assumptions that are applied to both sensor models. The alternating excitation field H is assumed to be homogeneous over the whole sample, with an amplitude of 10 mT μ_0^{-1} and an excitation frequency of $f=1$ kHz. The geometry of the excitation coil is therefore not included in both models. The amplitude of the excitation field is assumed to be low; for larger amplitudes the nonlinear magnetic properties of MNPs become important and the situation turns to the disadvantage of the detectability of MNPs. In the detected signal, the contribution from the excitation field is assumed to be effectively eliminated, *e.g.* by electronic compensation.

For tissue, the volume susceptibility of water $\chi_{tis} = -9.05 \times 10^{-6}$ is assumed, with 20% variation taking into account tissue differences ($-11 \times 10^{-6} < \chi_{tis} < -7 \times 10^{-6}$) [10]. For iron oxide ($Fe_3O_4$) MNPs the (optimistic) value of $\chi_{MNP} = 50$ is assumed. The respective mass densities are $\rho_{tis} = 1000$ kg m^{-3} and $\rho_{MNP} = 5180$ kg m^{-3}.

The detected voltage U (V) in the coil is the sum of the contributions from tissue and MNPs:

$$U = U_{tis} + U_{MNP}. \tag{1}$$

In practice, the tissue component can be eliminated by subtracting the signal U_{tis} of a tissue sample or region not containing MNPs ($U_{MNP}=0$). After this compensation procedure, the resulting response of tissues with MNPs can be fully attributed to the MNPs. However, because of the susceptibility variations of tissues in the human body, some uncertainty is introduced in the compensation, which affects the detectability of MNPs. This uncertainty can be expressed as a variability in the effective tissue susceptibility in the range of $\chi_{tis,var} = -4.0 \times 10^{-6}$. Because adequate reduction of this uncertainty during clinical procedures is difficult to verify, we use this full range of variability for the definition of the detection limit. For both sensor models, it is therefore assumed that the MNPs can be detected when the amplitude of the MNP contribution exceeds the signal variability of tissue: $U_{MNP} > -U_{tis,var}$.

2.1. Model A: sample volume enclosing coil

Sensor model A considers a setup typically for magnetic analysis of small (*ex vivo*) samples, with a coil that encloses the entire sample volume, containing the tissue and MNPs (Fig. 1). Assuming a detection coil with a homogeneous sensitivity profile in the coil, the whole sample space is assumed to be detected with a spatially constant coil sensitivity S (T A^{-1}), *i.e.* every sample volume element is detected with equal sensitivity. The space outside the coil is neglected in the signal contribution.

The signal U received by the detection coil can be written as

$$U = -2\pi f \cdot m \cdot S, \tag{2}$$

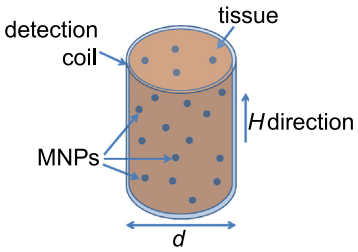

Fig. 1. Model A: a sample enclosing sensor with diameter d and a tissue volume which contains distributed MNPs. The tissue volume is assumed as a homogeneous medium, filling the entire coil volume. The sinusoidal excitation field is homogeneous and parallel to the axis of the coil.

with m (A m^2) being the magnetic moment of the entire sample. For the magnetic moment we write

$$m = M \cdot V = \chi \cdot H \cdot V, \tag{3}$$

with M (A m^{-1}) being the magnetization, V (m^3) the volume of sample material and H (A m^{-1}) the applied field. The detected voltage U is proportional to the total magnetic moment m of the sample. The individual susceptibilities of diamagnetic tissue and superparamagnetic MNP materials determine their respective partial contributions to the signal. According to the definition of MNP detectability, the MNPs are defined to be detectable if the magnetic moment of the MNPs m_{MNP} equals the opposite magnetic moment variability of the tissue $m_{tis,var}$:

$$m_{MNP} = -m_{tis,var} \longrightarrow \chi_{MNP} \cdot H \cdot V_{MNP} = -\chi_{tis,var} \cdot H \cdot V_{tis}. \tag{4}$$

Since the excitation field is assumed to be homogeneous, both the tissue and the MNPs are subjected to the same field. Thus, the susceptibilities of MNPs and tissue provide us the ratio of MNP and tissue volumes that produce the same magnetic moment:

$$\frac{V_{MNP}}{V_{tis}} = \frac{-\chi_{tis,var}}{\chi_{MNP}}. \tag{5}$$

Using the mass densities of tissue ρ_{tis} and iron oxide ρ_{MNP}, the mass ratio $\mathfrak{m}_{tis}$: $\mathfrak{m}_{MNP}$ of equally detected MNPs and tissue variations can be calculated:

$$\frac{\mathfrak{m}_{MNP}}{\mathfrak{m}_{tis}} = \frac{V_{MNP}}{V_{tis}} \frac{\rho_{MNP}}{\rho_{tis}}. \tag{6}$$

This mass ratio represents the minimum mass of iron oxide MNPs that can be detected in model A, with a tissue volume in the sample enclosing coil.

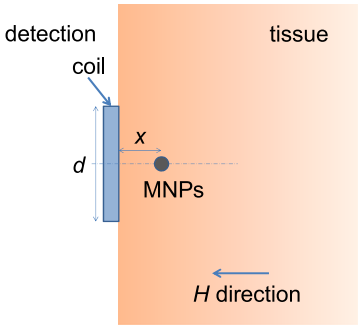

Fig. 2. Model B: the single sided sensor with diameter d and a tissue volume which contains a spot with MNPs. The tissue volume is assumed as a homogeneous infinite medium at the right side of the probe. The excitation field is homogeneous and parallel to the axis of the coil. The MNP spot is positioned on the axis of the coil at a distance x between 0 and 25 mm from the coil.

2.2. Model B: single sided detection of MNPs in a tissue volume

For *in vivo* applications with a clinical handheld MNP sensor, the sample volume is positioned at one side of the detection coil. Such a sensor is typically used in the search for clinically relevant MNP spots in tissue. A relatively large diamagnetic tissue volume is present, which contributes to the signal in the magnetometer. In this context, it is important whether the presence of a small volume of MNPs at a certain location can be determined. To obtain a quantitative indication for MNP detection with a single sided magnetometer, a model is defined with a single detection coil and an infinite, large tissue volume containing a small spot with MNPs (see Fig. 2).

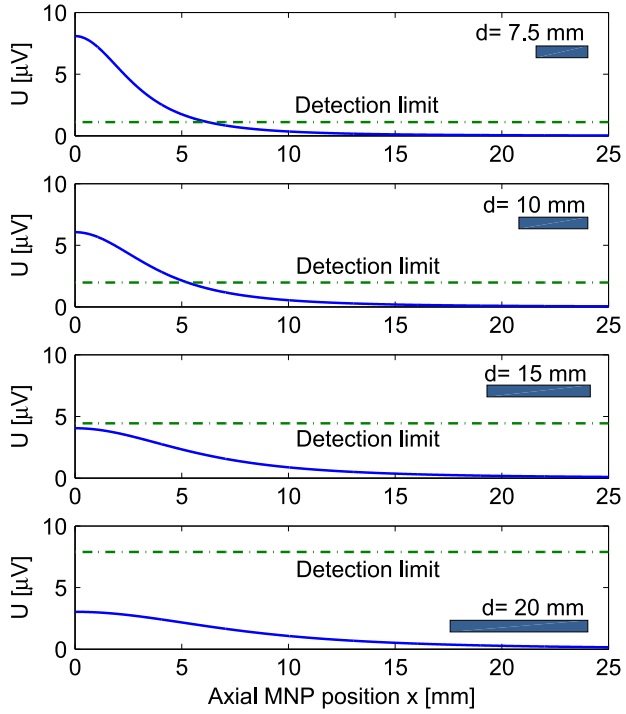

Fig. 3. The signal contribution U_{MNP} (blue solid line) for model B for different coil diameters calculated for a 1 µg iron oxide sample, plotted with the detection limit $U_{tis,var}$ defined by susceptibility variations of tissue (green dashed line). The calculated signals from tissue $U_{tis,var}$ and MNPs U_{MNP} are detected by a coil with 100 windings and a homogeneous excitation field of 10 mT alternating at $f=1$ kHz. Larger tissue volumes are detected with larger coil diameters, which reduces distant detection of MNPs. (For interpretation of the references to color in this figure caption, the reader is referred to the web version of this paper.)

In addition to the general assumptions mentioned above, some additional conditions are formulated. The detection coil has $n=100$ thin wired (~0.1 mm) windings, which justifies the assumption of zero coil length and a coil position $x=0$ m on the tissue surface. The spot with MNPs is positioned on the coil axis at different positions x. According to Eq. (1), the signal U received by the detection coil contains the individual contributions of the different materials in the sample. The signal contribution U_{tis} can be calculated using Faraday's law of induction. Since the tissue contribution is subtracted with the uncertainty of the variation in susceptibility, the remaining signal contribution that determines the detection limit is calculated by

$$U_{tis,var} = -n\frac{d\Phi_{tis,var}}{dt} = -n\frac{dB_{tis,var}}{dt}A, \tag{7}$$

with $\Phi_{tis,var}$ being the magnetic flux through the coil due to the magnetization variation of tissue and $A=\pi R^2$ (m^2) the coil surface. In this model, the tissue is assumed to be an infinite homogeneous medium at one side of the coil. The magnetization variation of the tissue $M_{tis,var}$ produces the magnetic field variation $B_{tis,var}$ that is detected by the sensing coil:

$$B_{tis,var} = \mu_0 M_{tis,var} = \mu_0 \cdot \chi_{tis,var} \cdot H. \tag{8}$$

The signal contribution U_{MNP} of 1 µg iron oxide MNPs depends on the position x on the axis of the detection coil and is calculated using Eqs. (2) and (3), assuming a homogeneous coil sensitivity $S(x)$ over the very small MNP volume. The coil sensitivity $S(x)$ is calculated using the Biot–Savart law, defined for the magnetic field strength on the axis of a single loop, divided by the applied current and multiplied by the number of turns:

$$S(x) = \frac{B(x)}{I} = \frac{n\mu_0 R^2}{2(R^2+x^2)^{3/2}}, \tag{9}$$

with B being the magnetic field at position x on the axis of a coil with diameter $d=2R$ (m) and I (A) the current through the coil. The spatially dependent coil sensitivity thus represents the field strength produced per unit current through the detection coil.

Assuming a homogeneous excitation field of $H=10$ mT μ_0^{-1}, the signal U_{MNP} of a small volume of MNPs containing 1 µg iron oxide at positions x between 0 and 25 mm on the coil axis and the uncertainty of the compensation signal for the tissue volume $U_{tis,var}$ are calculated. For a sensor with diameter $d=2R$, the detectable

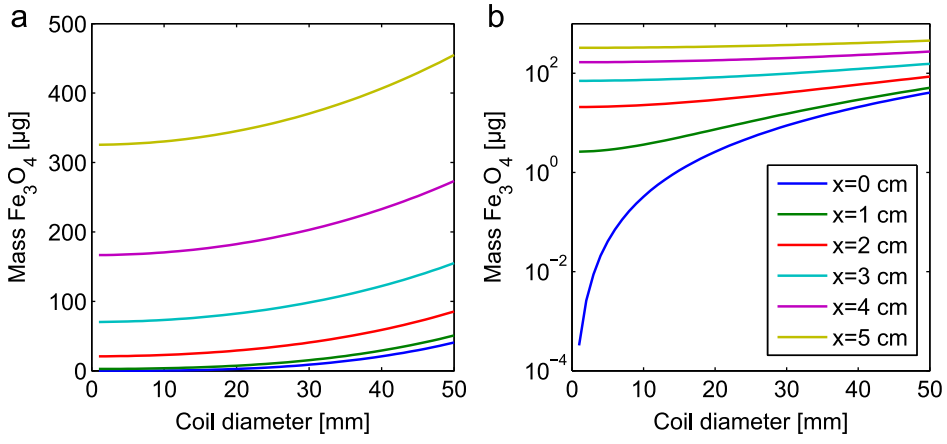

Fig. 4. The mass detection limit of model B for iron oxide MNPs in tissue vs. detection coil diameter, calculated for six axial distances to the coil. The mass detection limit increases rapidly with MNP distance and with coil diameter. For clarity, the mass values are plotted on linear (a) and logarithmic (b) scales.

iron oxide mass at position x is given by

$$\mathfrak{m}_{MNP} = 2\pi(R^2 + x^2)^{3/2}.\frac{-\chi_{tis,var}}{\chi_{MNP}}.\rho_{MNP}. \quad (10)$$

The iron oxide mass detection limit of sensors with diameters between 1 and 50 mm is calculated for 6 different MNP positions between 0 and 5 cm.

3. Results

3.1. Model A: sample volume enclosing coil

For the sample enclosing coil sensor, the detection limit of MNPs in tissue is reached for a volume ratio $V_{MNP}/V_{tis} = 4.0 \times 10^{-6}/50 = 8.0 \times 10^{-8}$. According to Eq. (6), this corresponds to a mass ratio of $\mathfrak{m}_{MNP}/\mathfrak{m}_{tis} = 8.0 \times 10^{-8}.5180/1000 = 4.1 \times 10^{-7}$. With model A, the iron oxide MNP mass that can be detected is 2.4 million times smaller than the contributing tissue mass. For successful iron oxide MNP detection with a sample enclosing coil, a 1 cm^3 tissue sample should contain at least 0.41 μg Fe_3O_4, equivalent to 0.30 μg iron.

3.2. Model B: single sided detection of MNPs in a tissue volume

For the surface sensor in model B, the results for four different coil diameters are shown in Fig. 3. The detection limit is determined by the voltage $U_{tis,var}$ that is produced by tissue with a susceptibility that is maximally different from the reference spot. As soon as the MNP contribution in the detected voltage decreases below the tissue variability contribution, the MNPs are regarded as undetectable. For example, for a coil with a diameter of 10 mm, 1 μg iron oxide nanoparticles can be detected up to a depth of 5 mm in tissue.

Similar to the calculations for a sample enclosing coil, the MNP detection limit increases with coil diameter, because the tissue contribution increases and the amplitude of the maximum MNP signal decreases. From Fig. 3, it is clear that the MNP signal of 1 μg iron oxide does not exceed the detection limit for coil diameters larger than approximately 15 mm, even if the MNPs are positioned close to the coil.

The detection limits for coil diameters between 0.1 and 5 cm and six different axial MNP positions are shown in Fig. 4. For example, using a large coil with a diameter of 5 cm, a minimum of about 41 μg iron oxide can be detected at the coil–tissue interface. At a distance of 5 cm, the MNP spot is only detectable if it contains more than 325 μg iron, even for the smallest coil.

4. Discussion and conclusions

The quantitative analysis of MNP detection, using a theoretical model of conventional alternating field magnetometry, has shown the limitations for clinical application. The variability of the diamagnetic susceptibility of tissue prohibits the detection of small MNP amounts deeply located in larger tissue volumes in patients.

For conventional alternating field magnetometry using a sample enclosing coil (model A) with a spatially homogeneous sensitivity, a homogeneous excitation field and compensated tissue contribution, the MNP detection limit is determined by the mass balance of MNPs and tissue. Under the most optimal conditions, the MNP mass that can be detected is 2.4 million times smaller than the contributing tissue mass. For very small tissue samples with relatively high MNP concentrations this might be acceptable. However, for larger tissue samples or cellular MNP uptake with typically low concentrations, this detection limit is insufficient for accurate sample analysis.

For the single sided detection coil in model B, only with small coils ($d < 15$ mm) and short MNP distances ($x < 7$ mm) the detectable iron oxide mass is below 1 μg. Thus for cases with superficial MNP locations, it is worth to consider small diameter coils. For deeply located MNP spots, the variability of tissue dominates over the response. For larger coil diameters the increased tissue contribution dominates over the MNP signal, even for close MNP positions.

The analysis was performed with specific assumptions that not only simplified the calculations, but also provided the most optimal conditions for sensitive MNP detection with a local probe. The assumption of a homogeneous detection field is the advantage of the MNP detection limit, since the MNP signal becomes less dependent on location. Especially for model B with the single sided detector, a single sided excitation coil would reduce the detection depth, since the spatial decay of the excitation field results in a reduced MNP magnetization and thus a lower MNP signal contribution.

The MNP detection limit derived from the tissue susceptibility variation is homogeneously applied to the modeled tissue volume. The detection limit may only decrease if the reference measurement can be performed with increased accuracy. Then, the tissue susceptibility of the reference tissue is similar to the tissue susceptibility around the MNPs. In surgical practice with a handheld probe it is difficult to improve the accuracy of the reference measurement, since probe placement on soft tissues is hardly reproducible. For cases with a larger variability in tissue susceptibility, the mass detection limit of MNPs increases, while the depth detection limit of the single sided probe in model B reduces.

The MNP susceptibility used for the calculations is based on what is found for a typical MRI contrast agent (Resovist). Although this value is optimistic, there are of course MNP formulations possible with a larger susceptibility. However, for biomedical applications it is unlikely to find materials for MNPs with a significantly larger susceptibility that would eliminate the limitations of conventional alternating field magnetometry.

The results presented above cannot be improved by choosing another amplitude or frequency of the excitation field. The results may even get worse, since the diamagnetic magnetization is frequency independent and linearly related to the excitation field, whereas the magnetic response of MNPs is strictly nonlinear and depends on the excitation frequency [11,12]. The assumption of a frequency independent linear MNP susceptibility in the present model is therefore the most optimistic case for MNP detection with conventional alternating fields. The geometric simplification of the single sided detection coil with zero length is the most sensitive design for a surface coil. For realistic, longer detection coils the sensitivity will decrease, which is the disadvantage of MNP detection.

The present quantitative analysis clearly shows that the conventional alternating field magnetometry approach for local MNP detection is limited by the significant contribution from tissue susceptibility variations. For a wide clinical acceptance of MNP detection in (surgical) interventions, a clinical probe is required which has a selective sensitivity for nonlinear MNPs. The probe should be able to detect micrograms iron oxide at a depth of several centimeters, by eliminating the linear magnetic contribution of tissue and exploiting the nonlinear properties of MNPs.

References

[1] M. Douek, J. Klaase, I. Monypenny, A. Kothari, K. Zechmeister, D. Brown, L. Wyld, P. Drew, H. Garmo, O. Agbaje, Q. Pankhurst, B. Anninga,

M. Grootendorst, B. Haken, M. Hall-Craggs, A. Purushotham, S. Pinder, Sentinel node biopsy using a magnetic tracer versus standard technique: The sentimag multicentre trial, Ann. Surg. Oncol. (2013) 1–9. http://dx.doi.org/10.1245/s10434-013-3379-6.

[2] M. Thill, A. Kurylcio, R. Welter, V. van Haasteren, B. Grosse, G. Berclaz, W. Polkowski, N. Hauser, The central-european sentimag study: sentinel lymph node biopsy with superparamagnetic iron oxide (SPIO) vs. radioisotope, The Breast 23 (2) (2014) 175–179. http://dx.doi.org/10.1016/j.breast.2014.01.004.

[3] T. Nakagawa, Y. Minamiya, Y. Katayose, H. Saito, K. Taguchi, H. Imano, H. Watanabe, K. Enomoto, M. Sageshima, T. Ueda, J.I. Ogawa, A novel method for sentinel lymph node mapping using magnetite in patients with non-small cell lung cancer, J. Thorac. Cardiovasc. Surg. 126 (2) (2003) 563–567, URL ⟨http://www.scopus.com/inward/record.url?eid=2-s2.0-0042856576&partnerID=40&md5=2d8af61a1f190921c229905e7bc90693⟩.

[4] Y. Minamiya, M. Ito, Y. Katayose, H. Saito, K. Imai, Y. Sato, J.I. Ogawa, Intraoperative sentinel lymph node mapping using a new sterilizable magnetometer in patients with nonsmall cell lung cancer, Ann. Thorac. Surg. 81 (1) (2006) 327–330, URL ⟨http://www.scopus.com/inward/record.url?eid=2-s2.0-29144485350&partnerID=40&md5=06636816b053f8ed9c2efd6dd10cae7c⟩.

[5] Y. Minamiya, M. Ito, Y. Hosono, H. Kawai, H. Saito, Y. Katayose, S. Motoyama, J.-I. Ogawa, Subpleural injection of tracer improves detection of mediastinal sentinel lymph nodes in non-small cell lung cancer, Eur. J. Cardio-Thorac. Surg. 32 (5) (2007) 770–775. http://dx.doi.org/10.1016/j.ejcts.2007.07.012.

[6] T. Ono, Y. Minamiya, M. Ito, H. Saito, S. Motoyama, H. Nanjo, J. Ogawa, Sentinel node mapping and micrometastasis in patients with clinical stage ia non-small cell lung cancer, Interact. Cardiovasc. Thorac. Surg. 9 (4) (2009) 659–661. http://dx.doi.org/10.1510/icvts.2009.214197.

[7] M. Shiozawa, S. Kobayashi, Y. Sato, H. Maeshima, Y. Hozumi, A. Lefor, K. Kurihara, N. Sata, Y. Yasuda, Magnetic resonance lymphography of sentinel lymph nodes in patients with breast cancer using superparamagnetic iron oxide: a feasibility study, Breast Cancer (2012) 1–8. http://dx.doi.org/10.1007/s12282-012-0401-y.

[8] M. Shiozawa, A. Lefor, Y. Hozumi, K. Kurihara, N. Sata, Y. Yasuda, M. Kusakabe, Sentinel lymph node biopsy in patients with breast cancer using superparamagnetic iron oxide and a magnetometer, Breast Cancer 20 (3) (2013) 223–229. http://dx.doi.org/10.1007/s12282-011-0327-9.

[9] C. Mathelin, S. Salvador, D. Huss, J.-L. Guyonnet, Precise localization of sentinel lymph nodes and estimation of their depth using a prototype intraoperative mini γ-camera in patients with breast cancer, J. Nucl. Med. 48 (4) (2007) 623–629. http://dx.doi.org/10.2967/jnumed.106.036574.

[10] J.F. Schenck, The role of magnetic susceptibility in magnetic resonance imaging: MRI magnetic compatibility of the first and second kinds, Med. Phys. 23 (6) (1996) 815–850. http://dx.doi.org/10.1118/1.597854.

[11] B.H. Erné, K. Butter, B.W.M. Kuipers, G.J. Vroege, Rotational diffusion in iron ferrofluids, Langmuir 19 (20) (2003) 8218–8225, URL ⟨http://www.scopus.com/scopus/inward/record.url?eid=2-s2.0-0142008833&partnerID=40⟩.

[12] T. Yoshida, K. Ogawa, K. Enpuku, N. Usuki, H. Kanzaki, AC susceptibility of magnetic fluid in nonlinear brownian relaxation region: experiment and comparison with numerical simulation, Jpn. J. Appl. Phys. 49 (5R) (2010) 053001. http://dx.doi.org/10.1143/JJAP.49.053001.